4-2019

A simplified LED-driven switch for fast-scan controlled-adsorption voltammetry instrumentation

Rhiannon Robke
University of South Carolina

Parastoo Hashemi
University of South Carolina

Eric Ramsson
Grand Valley State University, ramssone@gvsu.edu

HardwareX 5 (2019) e00051

Contents lists available at ScienceDirect

HardwareX

journal homepage: www.elsevier.com/locate/ohx

A simplified LED-driven switch for fast-scan controlled-adsorption voltammetry instrumentation

Rhiannon Robke [a], Parastoo Hashemi [a], Eric Ramsson [b,*]

[a] Department of Chemistry and Biochemistry, University of South Carolina, Columbia, SC, USA
[b] Department of Biomedical Science, Grand Valley State University, Allendale, MI, USA

ARTICLE INFO

Article history:
Received 11 May 2018
Received in revised form 26 December 2018
Accepted 27 December 2018

Keywords:
Dopamine
Fast-scan cyclic voltammetry
Basal
Circuit
Instrumentation
Component

ABSTRACT

Fast-scan cyclic voltammetry (FSCV) is an analytical tool used to probe neurochemical processes in real-time. A major drawback for specialized applications of FSCV is that instrumentation must be constructed or modified in-house by those with expertise in electronics. One such specialized application is the newly developed fast-scan controlled-adsorption voltammetry (FSCAV) that measures basal (tonic) *in vivo* dopamine and serotonin concentrations. FSCAV requires additional software and equipment (an operational amplifier coupled to a transistor-transistor logic) allowing the system to switch between applying a FSCV waveform and a constant potential to the working electrode. Herein we describe a novel, simplified switching component to facilitate the integration of FSCAV into existing FSCV instruments, thereby making this method more accessible to the community. Specifically, we employ two light emitting diodes (LEDs) to generate the voltage needed to drive a NPN bipolar junction transistor, substantially streamlining the circuitry and fabrication of the switching component. We performed *in vitro* and *in vivo* analyses to compare the new LED circuit vs. the original switch. Our data shows that the novel simplified switching component performs equally well when compared to traditional instrumentation. Thus, we present a new, simplified scheme to perform FSCAV that is cheap, simple, and easy to construct by individuals without a background in engineering and electronics.

Specifications table

Hardware name	*LED Circuit*
Subject area	• Chemistry and Biochemistry • Neuroscience • Biological Sciences (e.g. Microbiology and Biochemistry)
Hardware type	• Field measurements and sensors • Voltammetry
Open Source License	*Creative Commons Attribution-ShareAlike 3.0*
Cost of Hardware	~$7.00
Source File Repository	*N/A – design included in body of manuscript*

* Corresponding author.
E-mail address: ramssone@gvsu.edu (E. Ramsson).

https://doi.org/10.1016/j.ohx.2018.e00051
2468-0672/

1. Hardware in context

Fast-scan cyclic voltammetry (FSCV) is a powerful electrochemical tool that permits the identification and quantification of neurotransmitters on a sub-second timescale in both intact brain tissue and slice preparations [1,2]. Briefly, this technique employs carbon-fiber microelectrodes (CFMs) that attract small charged ions such as dopamine and serotonin during a short resting potential. An analyte-specific waveform is then applied to the CFM to induce electron transfer through the oxidation and reduction of the ion at discrete potentials (for review see [3]), which is measured as current vs. potential to obtain a cyclic voltammogram (CV). A CV acts as an electrochemical identifier and is used to qualify and quantify the analyte of interest [4]. Since the development of FSCV in the 1970's, numerous influential discoveries have been made on the role of dopamine in learning and motivation [5–7]. However, these breakthrough findings wouldn't have been possible without technological advancements in the data analysis and hardware employed in FSCV.

To permit the millisecond temporal resolution required to detect rapid neurochemical events, FSCV utilizes fast scan rates (up to 1000 V/s). These rapid measurements are attainable due to the early work of Howell et al., which recognized that the background charging current (resulting from fast scan rates) could be digitally-subtracted to reveal small, faradaic currents produced by monoamines of low, biologically-relevant concentrations [8]. More recently, analog background subtraction has been shown to be advantageous by enhancing the signal to noise ratio for longer recordings [9]. Developments in FSCV hardware have evolved to allow wireless recordings of neurotransmitters, greatly aiding behavioral studies in which the cable connection between the animal and recording equipment restricts the movement of animals [10,11]. To shed light on neuronal circuits, multi-electrode FSCV recordings have been established to record neurotransmitter activity from more than one brain region simultaneously in real-time [12,13]. A considerable effort has been made to couple powerful FSCV chemical recordings to other techniques such as electrophysiology to provide indispensable information on both presynaptic and postsynaptic events [14]. Stimulation artifacts, a traditional complication of FSCV recordings, have also been minimized using a neurochemical pattern generator system on a chip with switched-electrode management, allowing electrochemical events to be more clearly revealed [15]. With the intention of translating FSCV recordings to clinics, proof-of-principle studies showed Wireless Instantaneous Neurotransmitter Concentration System (WINCS) technology can be successfully integrated into existing human neurosurgical set-ups to reliably measure neurotransmission [16,17]. Although all of these studies have advanced the methods in which phasic chemical events can be measured, there is still a fundamental dearth of knowledge on basal (tonic) extracellular neurotransmitter concentrations on a rapid timescale.

In 2013, Atcherley et al. pioneered a cutting-edge voltammetric technique, termed fast-scan controlled-adsorption voltammetry (FSCAV) to enable a 10-second quantitative *in vivo* basal neurotransmitter recording [18]. FSCAV measurements are performed in three steps:

Step 1: the waveform is applied to the carbon-fiber microelectrode at high frequency (100 Hz) to minimize adsorption for 2 s.
Step 2: application of a constant potential for 10 s to allow the neurotransmitter to adsorb to the electrode surface, reaching a coverage density in equilibrium with the surroundings.
Step 3: the waveform is reapplied and the adsorbed neurotransmitter is measured with respect to the first step.

An advantage of utilizing FSCV with stimulated neurotransmitter release prior to FSCAV is the production of a CV, which is necessary to identify the analyte of interest and verify the functionality of the electrode placement. On its own, FSCAV requires signal convolution to produce a CV, something that is not possible in the *in vivo* milieu [19]. While incredibly powerful, FSCAV in its original incarnation required a CMOS precision analogue switch (ADG419; Analogue Devices) and custom software to switch between the triangle waveform and a constant voltage. Additionally, it required a PCIe-6341 National Instruments (NI) interface card for operation. Due to the custom software, more complicated wiring of the analogue switch, and differences in the NI interface card adopted by most systems [20,21], it remains difficult to integrate FSCAV into existing FSCV systems.

Here we present a simplified component, a LED circuit, which employs two light emitting diodes (LEDs) to generate the voltage needed to drive a NPN bipolar junction transistor in a straightforward manner to measure tonic neurotransmitter levels using FSCAV. This method has the advantage of being easy to manufacture and is easily implemented into existing FSCV platforms.

2. Hardware description

Those without prior electronic training may find it challenging to construct the original FSCAV switch. The new LED circuit described here requires just two infrared LEDs and one NPN transistor, enabling this alternative to be cost-effective and simple to construct with a basic understanding of soldering. LEDs were chosen due to their ability to act as photodiodes with the capacity to both emit and detect light. While other LEDs can be employed, we have had consistent results using infrared LEDs to generate the necessary voltage at the second LED. The ability to integrate the LED circuit into older FSCV systems is an additional advantage of this circuit.

The LED circuit achieves optical isolation of the signal by placing two infrared (890 nm; 4 V forward voltage) LEDs facing one another. If control of the circuit is occurring via the "Stim out" of existing systems, stimulation outputs are set at 4 V. If digital or transistor-transistor logic (TTL) pulses are used, a voltage divider can drop the standard 5 V to the necessary 4 V, as shown in Figs. 1–3 (R1 = 10 kOhm; R2 = 40 kOhm, for instance). The light from L1 will illuminate L2 and cause ~0.9 V to be generated at L2. This is enough to power the base of the NPN BJT transistor and allow the −0.4 V to pass. The output of the circuit is connected to the recording electrode, and when the −0.4 V is allowed to pass, the recording electrode is clamped at −0.4 V. The LED circuit provides the constant potential (-0.4 V) through one of two ways: 1) by connecting the circuit to an external power supply or 2) through National Instrument cards (e.g. 6052 or 6052e). To compare the design and application of the LED circuit to the original switch, please see the work conducted by Atcherley et al. in 2013 and 2015 [18,19].

The LED circuit:

- is a simplified, cheaper version of the original switch utilized in FSCAV
- can be coupled to older FSCV existing systems
- provides high temporal resolution measurements of tonic neurotransmitter concentrations

3. Design files

Design files summary

Design file name	File type	Open source license	Location of the file
Design file 1	*N/A*		*Included within the body of the manuscript.*

4. Bill of materials

Bill of Materials

Designator	Component	#	Cost per unit-currency	Total cost-currency	Source of materials	Material type
LED	OP295A Infrared 890 nm LED	2	$0.75	$1.50	Mouser Electronics	N/A
NPN Bipolar Transistor	BC548CTA NPN 30 V 100 mA	1	$0.20	$0.20	Mouser Electronics	N/A
BNC connector	565-6741 BNC female	1	$3.49	$3.49	Mouser Electronics	N/A
Resistor	588-53J10KE	1	$0.80	$0.80	Mouser Electronics	Wirewound
Resistors	71-CMF5540K000BHEB	1	$0.54	$0.54	Mouser Electronics	Metal thin-film

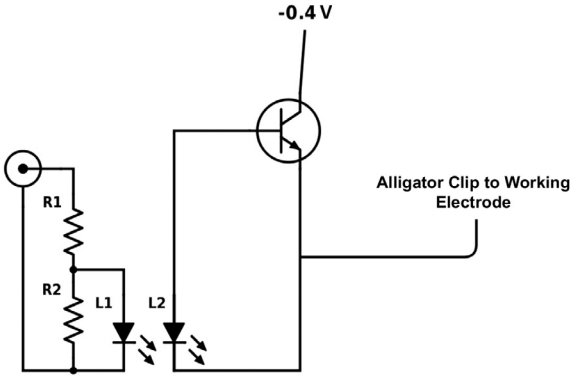

Fig. 1. Novel LED circuitry scheme. R1,2 = Resistors; L1,2 = LEDs. R1 = 10 kOhm, R2 = 40 kOhm, L1 and L2 = 890 nm, 4 V forward voltage. Transistor is NPN BJT.

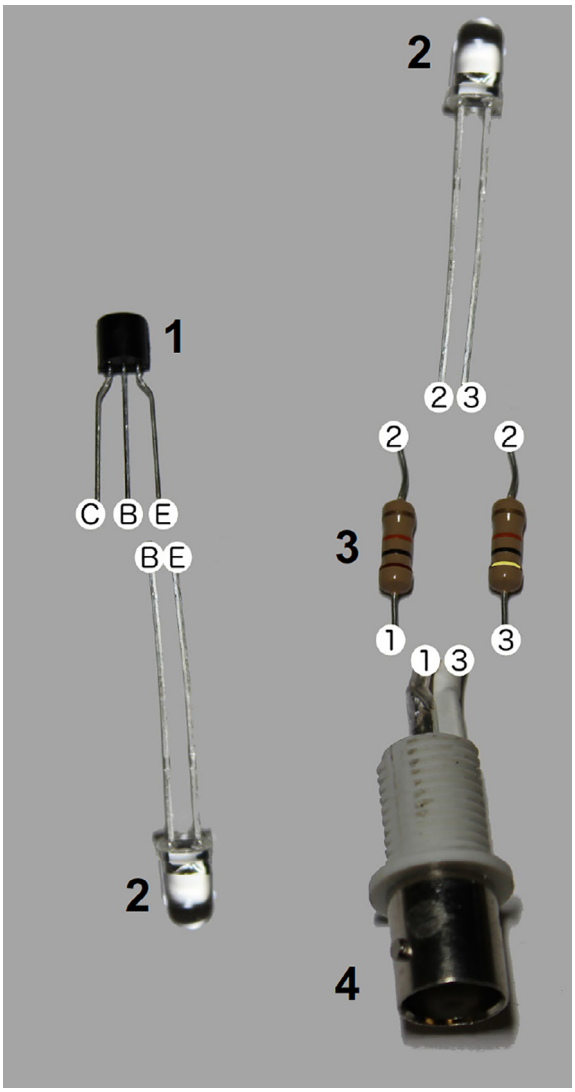

Fig. 2. Concise connection diagram. Same letters or numbers indicates soldering between those two connections. Bolded, black numbers correspond to the following: 1 = Transistor, 2 = LED, 3 = Resistor, 4 = BNC connector.

5. Build instructions

5.1. Breakdown instructions and tips for assembly

5.1.1. Purchase equipment listed in the table "bill of materials"

LED1 (L1) will receive 4 V to the anode from a TTL or National Instruments card 6052 (6052E) via a female BNC connector (see Section 6.1 for operation instructions). If receiving the standard 5 V from a TTL, a voltage divider is used to drop the voltage. R1 = 10 kOhm; R2 = 40 kOhm. The cathode is connected to ground.

5.1.2. Wire the components as shown in the schematic in Fig. 2

In the diagram, the parts with the same label are soldered together. The only two things not shown are the −0.4 V source, which connects to the C (collector) of the transistor and the output connecting to the working electrode, which connects to E (emitter). Please note that the flat end of the transistor faces away. The LEDs should be shrink-wrapped facing one another and/or surrounded by electrical tape to prevent stray light that can introduce noise. Isolating the LEDs in an opaque box may prove electrical tape unnecessary.

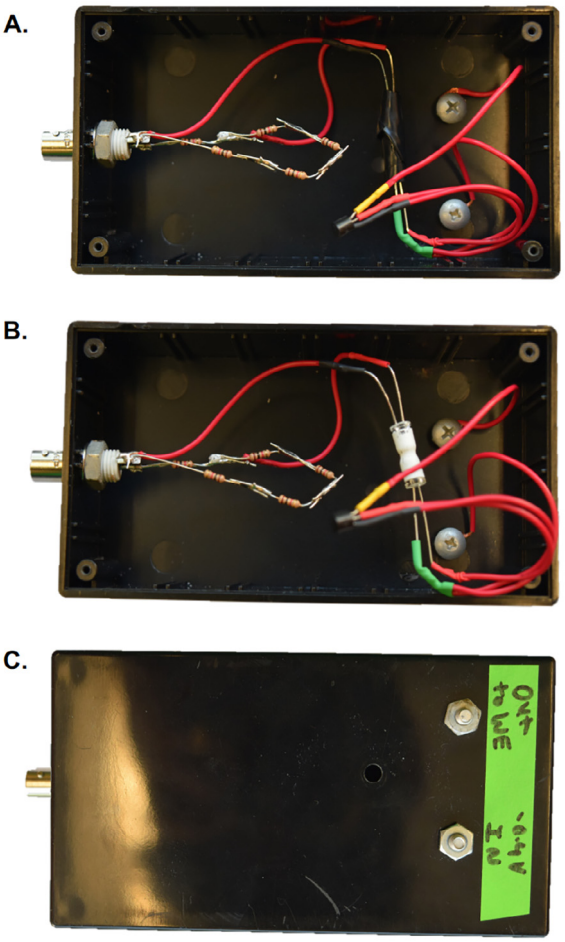

Fig. 3. Photographic representation of the LED circuit. **(A)** LEDs masked in electrical tape. **(B)** Reveal of LEDs (white component - shrink wrap). **(C)** Closed project box displaying the working electrode output (top screw) and the –0.4V input (bottom screw). **Notice 4 10 kOhm resistors (to create 40 kOhm) were used here (connected to TTL output; shown in both A and B).

5.1.3. Enclose the LED circuit in a project box as seen in Fig. 3

As seen in Fig. 3, screws are used as simple terminals. The −0.4 V input and working electrode output are connected to the associated screws. The collector of the NPN transistor will receive the −0.4 V input. Utilizing a project box assures that no stray light will reach the LEDs.

6. Operation instructions

6.1. Basic overview

The novel LED circuit scheme is shown in Fig. 1, with an external supply providing the 4 V to drive the two LEDs to power a NPN BJT transistor, enabling the −0.4 V to be applied to the carbon-fiber microelectrode (CFM) through an alligator clip. Alternating from the applied waveform to a constant potential is under the control of a TTL or "Stim out" via a BNC cable. The −0.4 V can come from an external power supply or from the 6052 or 6052e National Instruments cards of older FSCV systems. The −0.4 V power supply, when coming from the NI boards, originates from the second analog output (ao1). The first analog output (ao0) is utilized for the triangle wave output. A DC task for the −0.4 V output can be created in the National Instruments Automation Explorer. See below for how to get −0.4 V from your NI card:

1. Open up the Measurement and Automation Explorer.
2. On the left side find Devices and Interfaces and click on it (Fig. 4).
3. Click on the card of interest, in this case the 6052E (Fig. 5).
4. Click on Test Panels (Fig. 6).

5. Click on the Analog Output Tab.
6. Change the Channel Name to ao1 (ao0 is reserved for the triangle wave) (Fig. 7).
7. Leave the Mode as DC Value. Change the Output Value to −0.4 V (Fig. 8).
8. Click Update.
9. Connect a wire from the NI terminal pinouts (typically located within the Breakout Box) box for the 6052E (pin 21). On the other end connect an alligator clip. This will clip to the Collector of the NPN transistor.

6.2. Safety

Eye safety is advised while working with IR LEDs, since the beam is not visible to the human eye. However, the light beam should be contained when the circuit is powered due to shrink wrap and/or an opaque project box. Therefore, we do not foresee any potential safety hazards while setting up or utilizing our described circuit.

6.3. Operation

Through the use of FSCV software (WCCV or Demon Voltammetry, for example), FSCAV can be employed using the stimulation settings. Prior to data collection, each electrode is cycled using the dopamine FSCAV waveform (−0.4 V to 1.3 V at 1200 V s^{-1}) at 100 Hz for 10 min. For file collection, the pre-event time is set at 2 s, the event time at 10 s, and the entire file length at 30 s. During the 10 s event time, the LED circuit will act as a voltage clamp that will hold the working electrode at a constant potential of −0.4 V (or the resting potential of the analyte of interest), allowing the analyte to adsorb onto the carbon fiber electrode and reach equilibrium [19,22]. After file collection, analysis can be done by looking at the first background-subtracted dopamine cyclic voltammogram (CV). It is important to note that the first background-subtracted dopamine CV becomes visible on the 2nd or 3rd scan after the waveform is applied after the constant potential of 10 s. Data analysis must be conducted on the scan in which the first neurotransmitter peak becomes visible [22–24]. Due to electrode variability and slight alterations in the exact time point of the transition from constant potential to the waveform (+/- 10 ms), integration limits are visually adjusted per file.

7. Validation and characterization

7.1. In vitro FSCAV

To test agreement between FSCAV signals obtained with the switch and the LED circuit, a calibration was performed *in vitro* (n = 6 electrodes). Standard solutions of dopamine concentrations were prepared by dissolving dopamine hydrochlo-

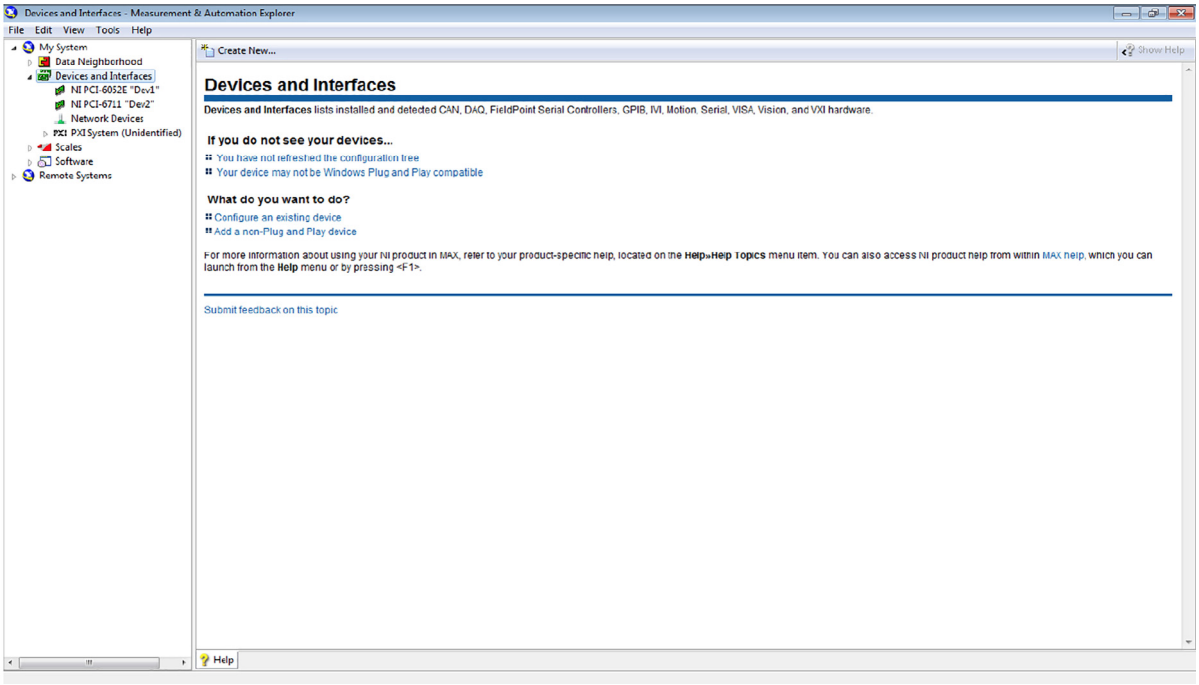

Fig. 4. Measurement and Automation Explorer: Devices and Interfaces.

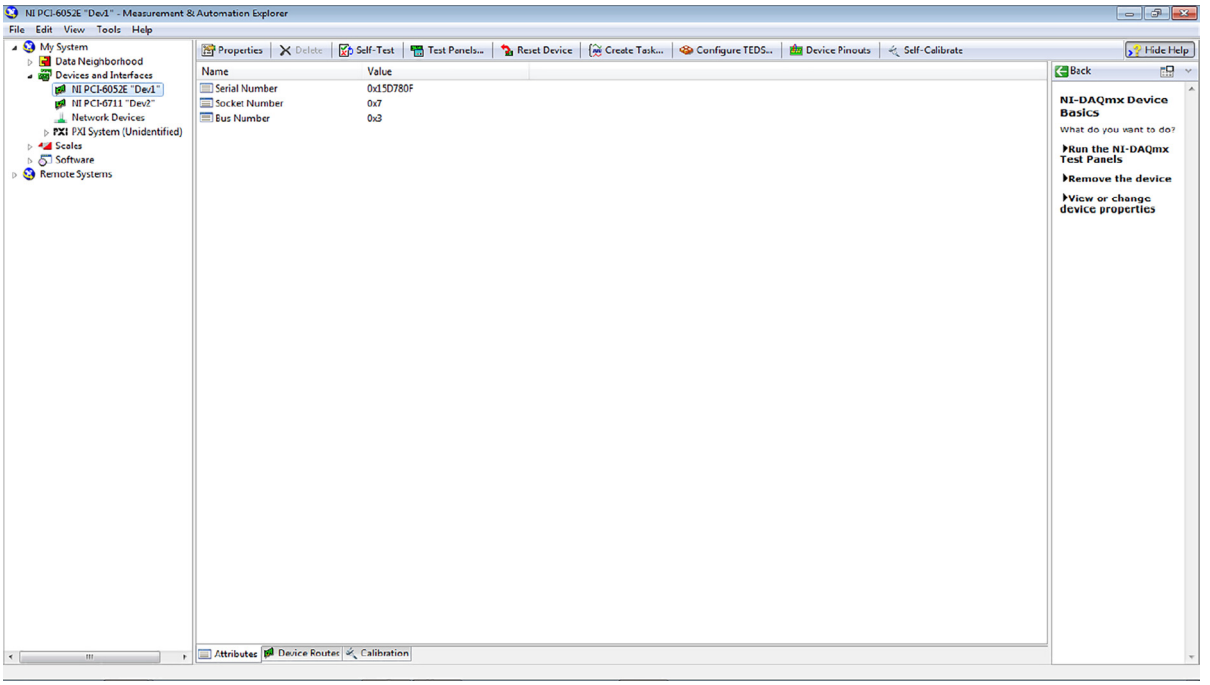

Fig. 5. NI card selection.

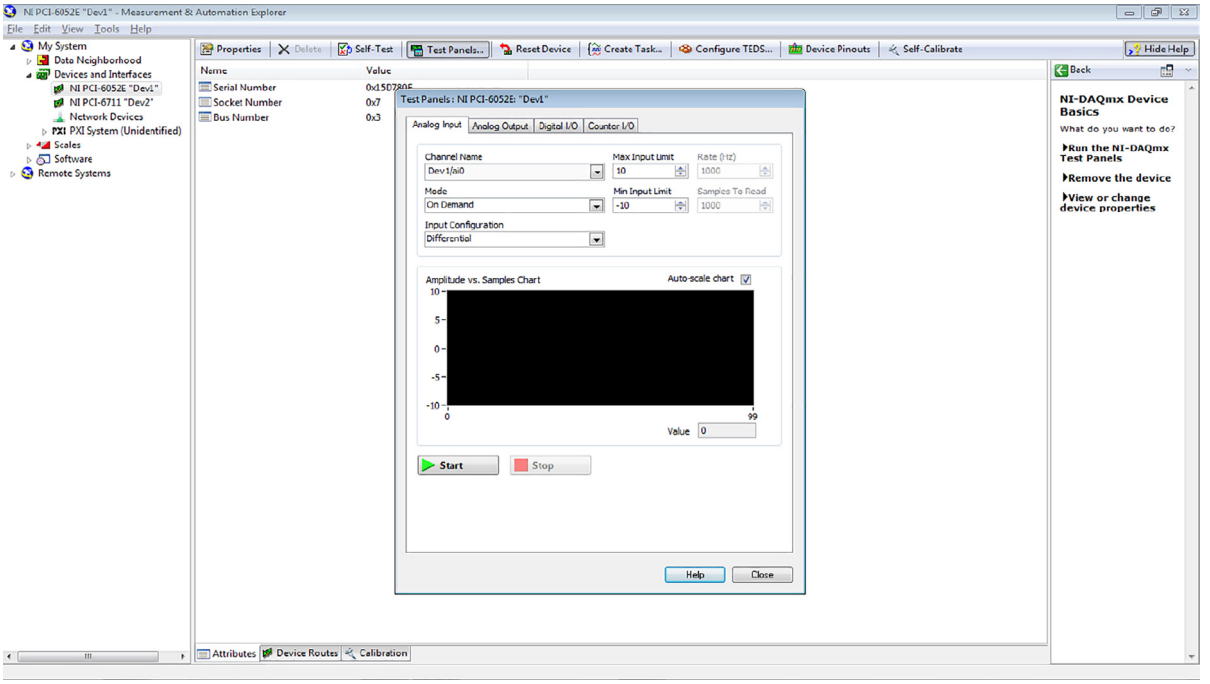

Fig. 6. Test Panel selection.

ride (Sigma-Aldrich, CO., MO, USA) in Tris Buffer (15 mM H_2NC-$(CH_2)(OH)_3$·HCl, 140 mM NaCl, 3.25 mM KCl, 1.2 mM $CaCl_2$, 1.25 mM NaH_2PO_4·H_2O, 1.2 mM $MgCl_2$, and 2.0 mM Na_2SO_4 at pH = 7.4 in deionized water). A calibration was performed using 50, 100, 200, and 500 nM dopamine concentrations using the dopamine FSCAV waveform. These concentrations were previously established to be within the linear calibration range for dopamine FSCAV [19,25]. The electrode was cycled using the dopamine FSCAV waveform at 100 Hz in Tris Buffer for 10 min before the same calibration was performed using the

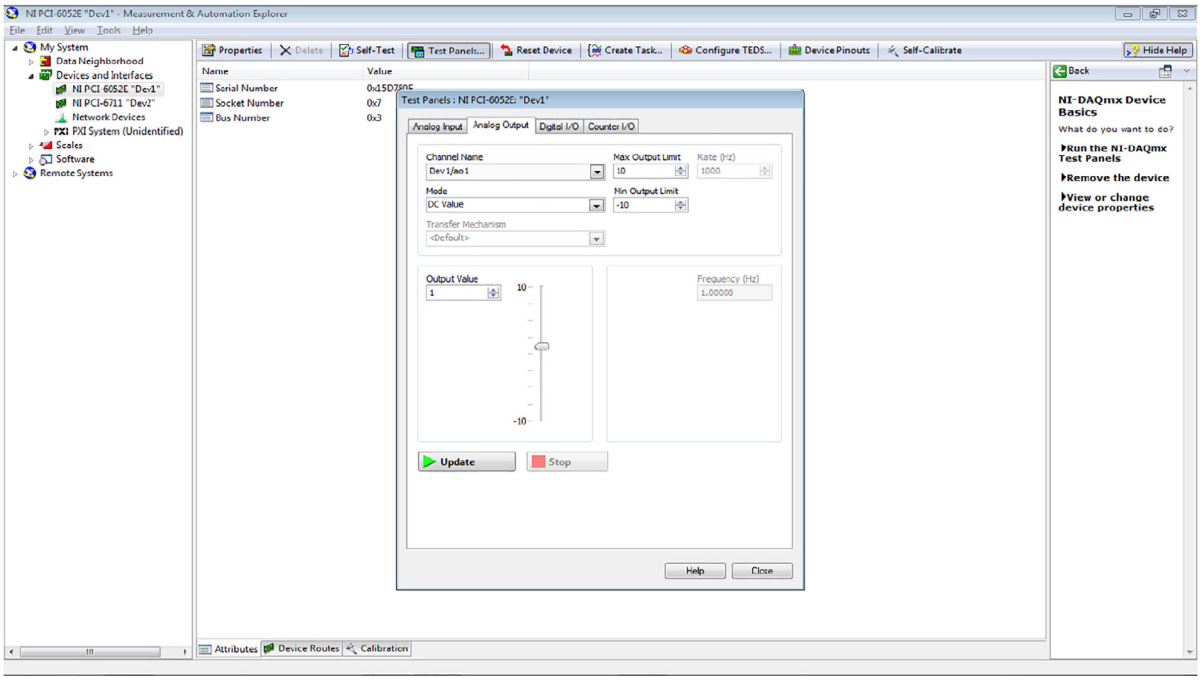

Fig. 7. Analog Output: change channel name to ao1.

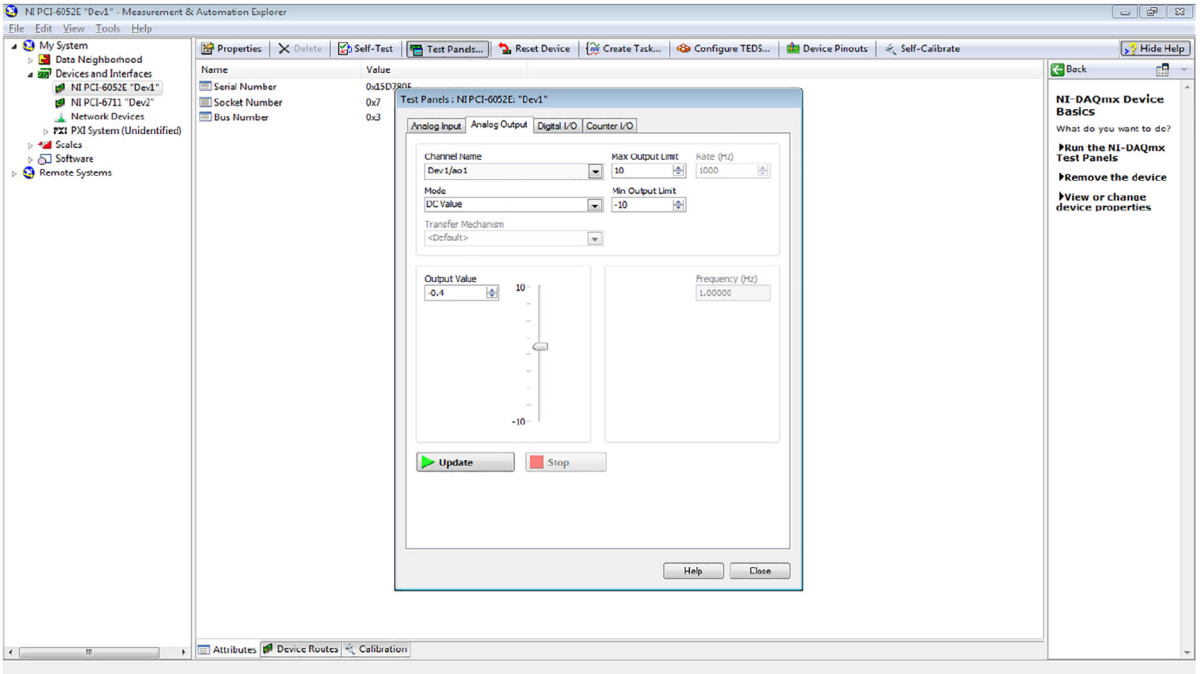

Fig. 8. Set output value to -0.4V.

other component. The initial component tested (LED or switch) was randomly assigned and altered between separate electrodes to reduce bias.

In Fig. 9A, representative FSCAV color plots obtained with the LED circuit and switch are shown. The color plots contain the voltage (vs. Ag/AgCl) on the y-axis, time (30 s) on the x-axis, and current (nA) is shown in false color. The three steps of FSCAV can be seen. **Step 1**: the waveform is applied to the carbon-fiber microelectrode at high frequency (100 Hz) to

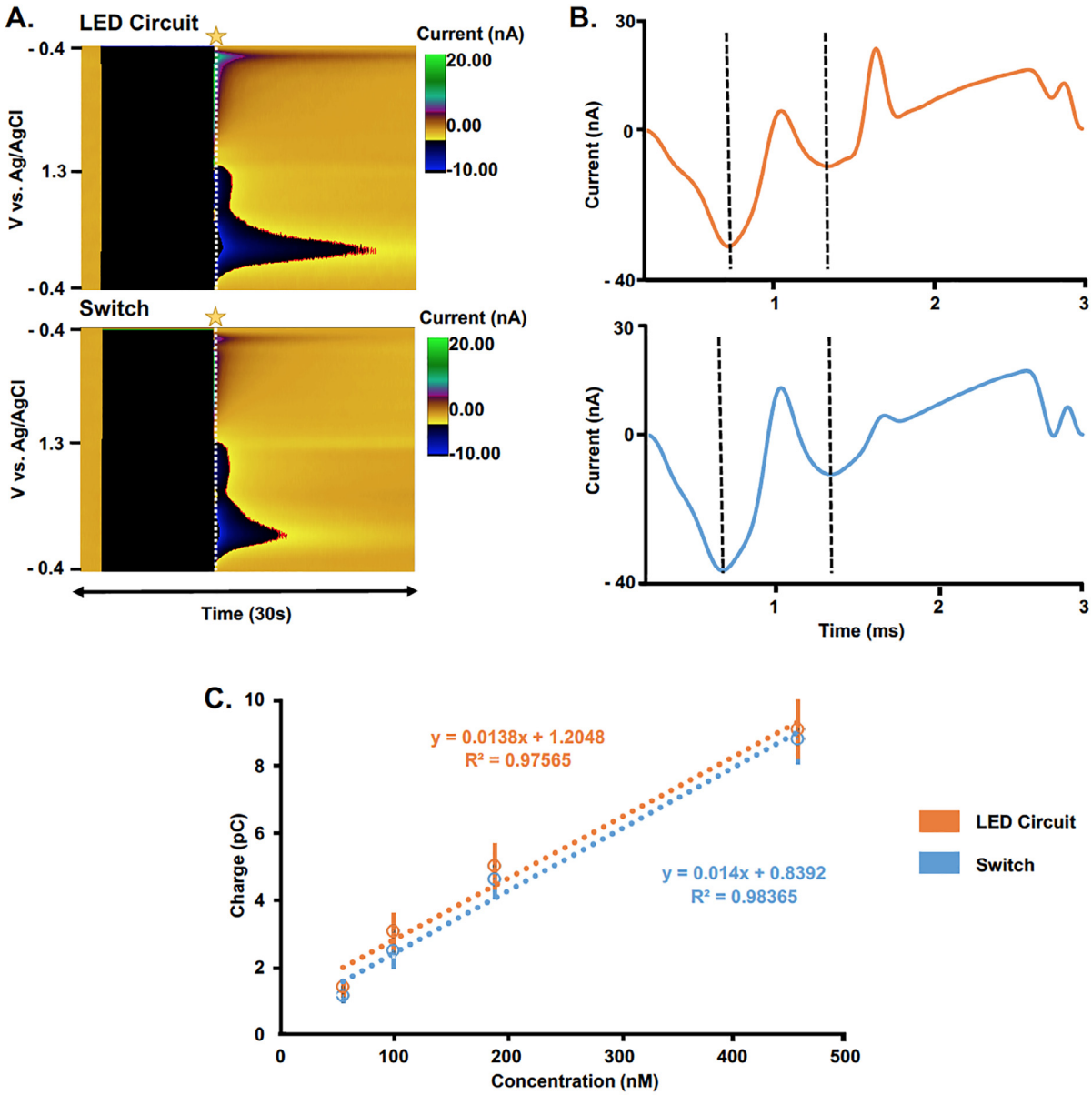

Fig. 9. In vitro calibration comparison of the LED circuit and original switch. **(A)** Representative color plots of LED circuit and switch files *in vitro*. **(B)** Extracted cyclic voltammograms from lateral color plots at dashed, starred line. Respective integration limits for the quantification of dopamine are shown as dashed, black lines for both the LED circuit (orange) and switch (blue). **(C)** Calibration curve and electrode response of the LED circuit and switch, showing no significant differences in their measurements (two way repeated measures ANOVA: n = 6 electrodes ± SEM).

minimize adsorption for 2 s (yellow, left side of pseudocolor plot). **Step 2**: a constant potential being applied for 10 s to allow the neurotransmitter to adsorb, reaching a coverage density in equilibrium with the surroundings (black area). **Step 3**: the waveform is reapplied and the adsorbed neurotransmitter is measured in respect to the first step (blue event area noted by the starred, dashed white line).

To compare measurements, the 3rd scan was utilized in each system when a clear, Faradaic dopamine peak was visible. Fig. 9**B** shows the respective current trace of the 3rd scan for the LED circuit (orange) and switch (blue) with current on the y-axis and time in milliseconds on the x-axis. The dashed lines note integration limits, or where the area under the curve was calculated, for the quantification of dopamine for each system.

To directly compare calibration data between the two systems, linear models relating charge to concentration are described. Fig. 9**C** reports the resulting averaged calibration plot of the LED circuit and switch with charge (pC) on the y-axis and concentration (nM) on the x-axis. Both systems are in agreement, with no statistical difference between linear

models from 50 to 500 nM of dopamine (two way repeated measures ANOVA (charge and concentration): $p > 0.05$, $n = 6$ electrodes ± SEM), a range consistent with expected *in vivo* concentrations [18].

7.2. In vivo FSCAV

After validating that the switch and the LED circuit enable statistically identical FSCAV measurements *in vitro*, we moved to comparisons of *in vivo* responses. *In vivo* dopamine measurements were performed in the nucleus accumbens core (NAcc), a brain locality rich in dopamine terminals [26,27]. Handling and surgery of 3 male C57BL/6J mice weighing 20–25 g (Jackson Laboratory, Bar Harbor, ME) were in agreement with The Guide for the Care and Use of Laboratory Animals and approved by the Institutional Animal Care Use Committee for South Carolina University. Urethane (25% dissolved in 0.9% NaCl solution, Hospira, Lake Forest, IL) was administered via intraperitoneal (*i.p.*) injection and stereotaxic surgery (David Kopf Instruments, Tujunga, CA) was performed. A heating pad sustained mouse body temperature around 37 °C (Braintree Scientific, Braintree, MA).

First, to verify that the electrode was correctly placed in the NAcc, stimulation of the medial forebrain bundle (MFB) was used to confirm the release of dopamine with FSCV using a triangular waveform (−0.4 V to 1.3 V at 400 V s^{-1}). Stereotaxic

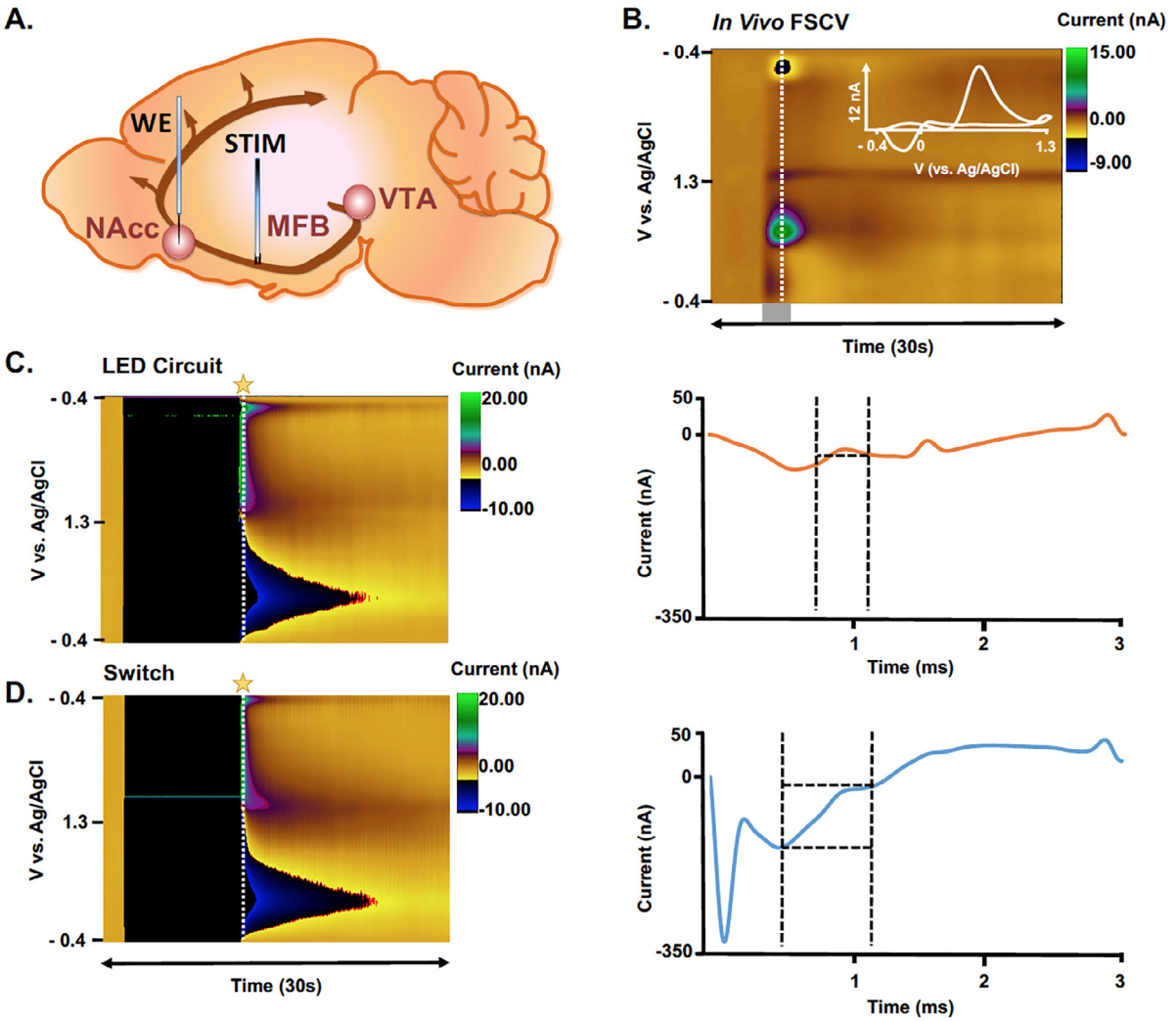

Fig. 10. In vivo comparison of novel LED circuit and original switch. **(A)** Scheme of *in vivo* experiment set-up in the mouse brain. WE = working electrode, STIM = stimulating electrode, NAcc = nucleus accumbens core, MFB = medial forebrain bundle, VTA = ventral tegmental area. **(B)** FSCV *in vivo* recording verifying dopamine release in the NAcc after electrical stimulation of the MFB. **(C)** LED circuit color plot and extracted cyclic voltammogram from the white, dashed, starred line (3rd scan after waveform is reapplied). Integration limits are shown with cross hairs of the two limits aligned under the peak (black, dashed lines). **(D)** Switch color plot and extracted cyclic voltammogram from the white, dashed, starred line (2nd scan after waveform is reapplied). Integration limits are shown in black, dashed lines.

coordinates were taken in reference to bregma. A Nafion-coated CFM was inserted into the nucleus accumbens core (NAcc) (AP: +1.09, ML: −1.25, DV: −4.30). 120 Biphasic pulses were applied to the medial forebrain bundle (MFB) (AP: −1.58, ML: −1.00, DV: −4.80) through a linear constant current stimulus isolator (NL800A, Neurolog, Medical Systems Corp., Great Neck, NY). An Ag/AgCl reference electrode was implanted into the brain's opposite hemisphere.

Fig. 10**A (top left)** displays the experimental scheme, noting the working electrode in the NAcc and the stimulating electrode in the MFB. Fig. 10**B** shows the *in vivo* FSCV color plot, in which the green event denotes the release of dopamine by stimulation (grey bar below – 2 s duration). Dopamine is confirmed by its distinctive cyclic voltammogram; oxidation at 0.6 V and reduction at −0.2 V (white inset taken from the vertical, dashed white line).

Next, the dopamine FSCAV waveform was applied to the working electrode and the two FSCAV equipment schemes were compared. The scheme used (switch or LED circuit) to obtain initial *in vivo* measurements was alternated between animals as a control. Fig. 10**C** shows the LED circuit *in vivo* color plot and corresponding current trace for the 3rd scan, shown by the star and dashed, white line. The integration limits are set by first placing the final limit where a stable minimum can be found after the oxidative peak, and then lining up the cross hairs of the initial limit to the final (Fig. 10**C**). It is important to note that the 2nd scan could not be taken for the LED Circuit, as the background, governed by capacitive current, was large enough (∼600 nA) to mask the Faradaic peaks, most likely because of stray capacitance from the BJT transistor. In Fig. 10**D**, a color plot and current trace are shown for the original switch. For the switch's integration limits, we utilize the 2nd scan (shown by the star and white dashed line), as previously published [19]. While this scan has a large, non-Faradaic background peak (∼350 nA), most importantly, the 2nd scan is used for analysis because it contains the first clearly distinguishable Faradaic dopamine response.

The original FSCAV work applied convolution theory prior to analysis [18,25], however, it has since been shown that this is not feasible *in vivo* [22–24]. As such, we did not employ convolution theory for our data analysis; integration was sufficient to compare the two equipment schemes. The switch's integration limits are set by placing both initial and final limits at the local minima, and encompassing the entire peak. It is important to note that the integration limits *in vivo* were altered from the previous *in vitro* comparison of both systems to account for the complex matrix of the brain and additional interfering analytes that are present [28–30]. While it is not entirely clear why the two systems differ in their response to the *in vivo* matrix (requiring 2nd vs. 3rd scan), it is important to note that the new LED circuit is capable of detecting basal dopamine levels. Since we are using the 2nd scan for the switch [19], and the 3rd scan for the LED circuit (described above), the integration limits between the two differ greatly. However, similar *in vivo* basal dopamine concentrations are found. Since our measurements are collected on a rapid timescale of 100 Hz and data is extracted by identifying the first visible neurotransmitter peak for both systems, the difference in concentration between the 2nd vs. 3rd scan is negligible.

Using the same calibration procedure as the *in vitro* experiment, fitted linear models were obtained and estimates of *in vivo* dopamine concentrations were found to be 95.0 ± 11.0 nM for the switch and 94.4 ± 7.0 nM for the novel LED circuit. These values are statistically identical and in good agreement with values that we previously published [19] (student *t* test: $p > 0.05$, $n = 3$ mice ± SEM).

As a final characterization, the root-mean-square signal to noise ratio (RMS SNR) of the *in vivo* recordings was calculated. We performed our RMS SNR calculation using the 3rd scan of the LED circuit vs. the 2nd scan for the switch and obtained the signal and noise readouts from custom software (WCCV 3.06, written in LabView 2014 by Knowmad Technologies, LLC, Tucson, AZ, USA). The resulting RMS SNR was 281.7 for the LED circuit and 562.6 for the switch. It is important to note that during the 2nd scan for the switch, there is a large peak which contributes to the signal, as shown in the current vs. time (IT) curve in Fig. 10**D**. However, as previously mentioned, since the first, clear dopamine peak is also obtained during the 2nd scan, this scan is feasible to obtain *in vivo* concentrations of dopamine. Due to the RMS SNR values and the requirement to use the 3rd scan for the LED circuit data analysis, we conclude the BJT transistor that is utilized by the LED system takes longer to shut off and may add stray capacitance that appears as additional background. The CMOS precision switch has a much faster switching capability, enabling the dopamine peak to already appear by the 2nd scan. However, overall, the LED circuit provides high enough S/N for *in vivo* measurements with accurate results and is both easier and cheaper to construct.

Conflict of interest

The authors declare no conflict of interest.

Acknowledgements

This work was supported by the National Institute of Health [MH106563].

References

[1] D.L. Robinson, B.J. Venton, M.L. Heien, R.M. Wightman, Detecting subsecond dopamine release with fast-scan cyclic voltammetry in vivo, Clin. Chem. 49 (10) (2003) 1763–1773.
[2] C.E. John, S.R. Jones, Voltammetric characterization of the effect of monoamine uptake inhibitors and releasers on dopamine and serotonin uptake in mouse caudate-putamen and substantia nigra slices, Neuropharmacology 52 (8) (2007) 1596–1605.
[3] J.G. Roberts, L.A. Sombers, Fast-scan cyclic voltammetry: chemical sensing in the brain and beyond, Anal. Chem. 90 (1) (2017) 490–504.

[4] P.E.M. Phillips, R.M. Wightman, Critical guidelines for validation of the selectivity of in-vivo chemical microsensors, Trends Anal. Chem. 22 (9) (2003) 509–514.
[5] R.N. Adams, Probing brain chemistry with electroanalytical techniques, Anal. Chem. 48 (14) (1976) 1126A–1138A.
[6] P.E.M. Phillips, D.L. Robinson, G.D. Stuber, R.M. Carelli, R.M. Wightman, Real-time measurements of phasic changes in extracellular dopamine concentration in freely moving rats by fast-scan cyclic voltammetry, in: Drugs of Abuse, Humana Press, 2003, pp. 443–464.
[7] S.B. Flagel, J.J. Clark, T.E. Robinson, L. Mayo, A. Cruzi, I. Willuhn, C.A. Akers, S.M. Clinton, P.E.M. Phillips, H. Akil, A selective role for dopamine in stimulus-reward learning, Nature 469 (7328) (2011) 53.
[8] J.O. Howell, W.G. Kuhr, R.E. Ensman, R.M. Wightman, Background subtraction for rapid scan voltammetry, J. Electroanal. Chem. 209 (1) (1986) 77–90.
[9] A. Hermans, R.B. Keithley, J.M. Kita, L.A. Sombers, R.M. Wightman, Dopamine detection with fast-scan cyclic voltammetry used with analog background subtraction, Anal. Chem. 80 (11) (2008) 4040–4048.
[10] P.A. Garris, R. Ensman, J. Poehlman, A. Alexander, P.E. Langley, S.G. Sandberg, P.G. Greco, R.M. Wightman, G.V. Rebec, Wireless transmission of fast-scan cyclic voltammetry at a carbon-fiber microelectrode: proof of principle, J. Neurosci. Methods 140 (1–2) (2004) 103–115.
[11] M. Roham, C.D. Blaha, P.A. Garris, K.H. Lee, P. Mohseni, A configurable IC for wireless real-time in vivo monitoring of chemical and electrical neural activity, in: 2009 Annual International Conference of the IEEE Engineering in Medicine and Biology Society (2009) 4222–4225.
[12] M.K. Zacheck, P. Takmakov, J. Park, R.M. Wightman, G.S. McCarty, Simultaneous monitoring of dopamine concentration at spatially different brain locations in vivo, Biosens. Bioelectron. 25 (5) (2010) 1179–1185.
[13] M.E. Fox, M.A. Mikhailova, C.E. Bass, P. Takmakov, R.R. Gainedinov, E.A. Budygin, R.M. Wightman, Cross-hemispheric dopamine projections have functional significance, Proc. Natl. Acad. Sci. 113 (25) (2016) 6985–6990.
[14] P. Takmakov, C.J. McKinney, R.M. Carelli, R.M. Wightman, Instrumentation for fast-scan cyclic voltammetry combined with electrophysiology for behavioral experiments in freely moving animals, Rev. Sci. Instrum. 82 (7) (2011) 074302.
[15] B. Bozorgzadeh, D.P. Covey, C.D. Howard, P.A. Garris, P. Mohseni, A neurochemical pattern generator SoC with switched-electrode management for single-chip electrical stimulation and 9.3 uW, 78 pA rms, 400 V/s FSCV sensing, IEEE J. Solid-State Circuits 49 (4) (2014) 881–895.
[16] C.J. Griessenauer, S.Y. Chang, S.J. Tye, C.J. Kimble, K.E. Bennet, P.A. Garris, K.H. Lee, WINCS-based wireless electrochemical monitoring of serotonin (5-HT) using fast-scan cyclic voltammetry: proof of principle, J. Neurosurg. 113 (3) (2010) 656.
[17] S.Y. Chang, T. Jay, J. Munoz, I. Kim, K.H. Lee, Wireless fast-scan cyclic voltammetry measurement of histamine using WINCS—a proof-of-principle study, Analyst 137 (9) (2012) 2158–2165.
[18] C.W. Atcherley, N.D. Laude, K.L. Parent, M.L. Heien, Fast-scan controlled-adsorption voltammetry for the quantification of absolute concentrations and adsorption dynamics, Langmuir 29 (48) (2013) 14885–14892.
[19] C.W. Atcherley, K.M. Wood, K.L. Parent, P. Hashemi, M.L. Heien, The coaction of tonic and phasic dopamine dynamics, Chem. Commun. 51 (12) (2015) 2235–2238.
[20] E.S. Bucher, K. Brooks, M.D. Verber, R.B. Keithley, C. Owesson-White, S. Carroll, P. Takmakov, C.J. McKinney, R.M. Wightman, Flexible software platform for fast-scan cyclic voltammetry data acquisition and analysis, Anal. Chem. 85 (21) (2013) 10344–10353.
[21] J.T. Yorgason, R.A. España, S.R. Jones, Demon voltammetry and analysis software: analysis of cocaine-induced alterations in dopamine signaling using multiple kinetic measures, J. Neurosci. Methods 202 (2) (2011) 158–164.
[22] A. Abdalla, C.W. Atcherley, P. Pathirathna, S. Samaranayake, B. Qiang, E. Pena, S.L. Morgan, M.L. Heien, P. Hashemi, In vivo ambient serotonin measurements at carbon-fiber microelectrodes, Anal. Chem. 89 (18) (2017) 9703–9711.
[23] M.H. Burrell, C.W. Atcherley, M.L. Heien, J. Lipski, A novel electrochemical approach for prolonged measurement of absolute levels of extracellular dopamine in brain slices, ACS Chem. Neurosci. 6 (11) (2015) 1802–1812.
[24] P. Pathirathna, T. Siriwardhane, S.P. McElmurry, S.L. Morgan, P. Hashemi, Fast voltammetry of metals at carbon-fiber microelectrodes: towards an online speciation sensor, Analyst 141 (23) (2016) 6432–6437.
[25] C.W. Atcherley, N.D. Laude, E.B. Monroe, K.M. Wood, P. Hashemi, M.L. Heien, Improved calibration of voltammetric sensors for studying pharmacological effects on dopamine transporter kinetics in vivo, ACS Chem. Neurosci. 6 (9) (2014) 1509–1516.
[26] M.J. Nirenberg, J. Chan, A. Pohorille, R.A. Vaughan, G.R. Uhl, M.J. Kuhar, V.M. Pickel, The dopamine transporter: comparative ultrastructure of dopaminergic axons in limbic and motor compartments of the nucleus accumbens, J. Neurosci. 17 (18) (1997) 6899–6907.
[27] G.E. Meredith, R. Agolia, M.P.M. Arts, H.J. Groenewegen, D.S. Zahm, Morphological differences between projection neurons of the core and shell in the nucleus-accumbens of the rat, Neuroscience 50 (1) (1992) 149–162.
[28] P. Takmakov, M.K. Zachek, R.B. Keithley, E.S. Bucher, G.S. McCarty, R.M. Wightman, Characterization of local pH changes in brain using fast-scan cyclic voltammetry with carbon microelectrodes, Anal. Chem. 82 (23) (2010) 9892–9900.
[29] P.S. Cahill, Q.D. Walker, J.M. Finnegan, G.E. Mickelson, E.R. Travis, R.M. Wightman, Microelectrodes for the measurement of catecholamines in biological systems, Anal. Chem. 68 (18) (1996) 3180–3186.
[30] M.L. Heien, M.A. Johnson, R.M. Wightman, Resolving neurotransmitters detected by fast-scan cyclic voltammetry, Anal. Chem. 76 (19) (2004) 5697–5704.